Direct Observation of Node-to-Node Communication in Zeolitic Imidazolate Frameworks

Brian Pattengale,[a] Daniel J. SantaLucia,[b] Sizhuo Yang,[a] Wenhui Hu,[a] Cunming Liu,[c] Xiaoyi Zhang,[c] John F. Berry,[b]* and Jier Huang[a]*

[a]Department of Chemistry, Marquette University, Milwaukee, Wisconsin, 53201

[b]Department of Chemistry, University of Wisconsin, Madison, Wisconsin, 53706

[c]X-ray Science Division, Argonne National Laboratory, Argonne, Illinois, 60349

Supporting Information Placeholder

ABSTRACT: Zeolitic imidazolate frameworks (ZIFs) with open-shell transition metal nodes represent a promising class of highly-ordered light harvesting antennas for photoenergy applications. However, their charge transport properties within the framework, the key criterion to achieve efficient photoenergy conversion, are not yet explored. Herein, we report the first direct evidence of a charge transport pathway through node-to-node communication in both ground state and excited state ZIFs using the combination of paramagnetic susceptibility measurements and time resolved optical and X-ray absorption spectroscopy. These findings provide unprecedented new insights into the photoactivity and charge transport nature of ZIF frameworks, paving the way for their novel application as light harvesting arrays in diverse photoenergy conversion devices.

In natural photosynthesis, a highly-ordered architecture composed of light-harvesting pigments plays the key role of light absorption and subsequent energy migration to the reaction centers.[1] Inspired from nature, an artificial photocatalytic system to generate solar fuels requires the utility of ordered chromophore assemblies as efficient light harvesting antennas. Metal-organic frameworks (MOFs), an emerging class of porous crystalline materials that can precisely arrange chromophores through ordered ligand-to-metal coordination, represent excellent platforms as light harvesting antennas.[2-15] A particularly interesting subclass of such light harvesting MOFs are zeolitic imidazolate frameworks (ZIFs),[16-18] which were recently identified to have intrinsic photophysical properties with broad absorption across UV-visible and near IR spectral region and an exceptionally long-lived excited state (~ 2.9 μs lifetime).[19-21] More interestingly, this long-lived excited state was found to be an excited charge separated (ECS) state that can be dissociated through electron transfer to an organic species,[22] showing enormous promise toward the application of ZIFs as next generation light harvesting and energy delivery antennas for solar energy conversion.

A judicious question that emerged following the discovery of the long-lived ECS state is whether this state can undergo facile charge transport across a ZIF framework, a key criterion to achieve efficient photoenergy conversion. Recent theoretical studies reported the electronic structure of ZIFs; the d orbitals

Scheme 1. Schematic representation of mixed-metal ZIF-67

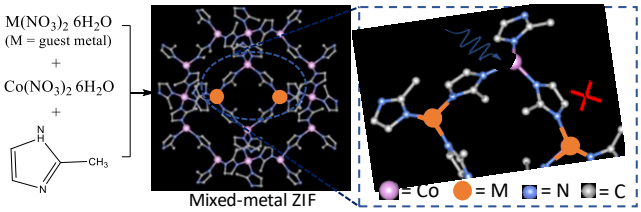

of the metal nodes can be conceived as comprising a continuous band,[23-26] in agreement with the improved conductivity in Co^{2+}-based ZIFs with respect to highly resistive closed-shell Zn^{2+}-based ZIFs.[27] While such exploratory work implies the possibility of charge transport via metal nodes in ZIFs, it is essential to establish an original approach to seek direct evidence of the charge transport mechanism experimentally.

Herein, we uncover the nature of charge transport in ZIF materials using advanced spectroscopic methods. We designed mixed-metal isostructural ZIFs (Scheme 1) by introducing a guest metal to the ZIF-67 parent framework (which has Co^{2+} at the metal nodes connected by 2-methyl imidazolate linkers). We hypothesized that a guest metal would perturb the ECS dynamics if charge transport occurs within the ZIF framework; redox-inert metals (such as Zn^{2+}) incorporated into the framework may prevent charge transport while redox-active guest metals (such as Cu^{2+}) may facilitate charge transport through metal-to-metal charge transfer (MMCT) pathways. Using the combination of paramagnetic susceptibility measurements (obtained via a SQUID), optical transient absorption (OTA), and X-ray transient absorption (XTA) spectroscopy to directly probe the interplay between the guest and parent metals within the parent framework, we not only show the first-ever reported intrinsic antiferromagnetic ordering of metal nodes in ground state ZIFs but also demonstrate direct evidence of charge transport through node-to-node communication in photoexcited ZIFs.

The mixed-metal ZIFs were synthesized by incorporating controlled amounts of Zn^{2+} salts and Cu^{2+} salts into Co^{2+} salts (X%M@ZIF-67; X=the percent of guest metal; M=guest metal) in the presence of 2-methylimidazole (Scheme 1), in contrast

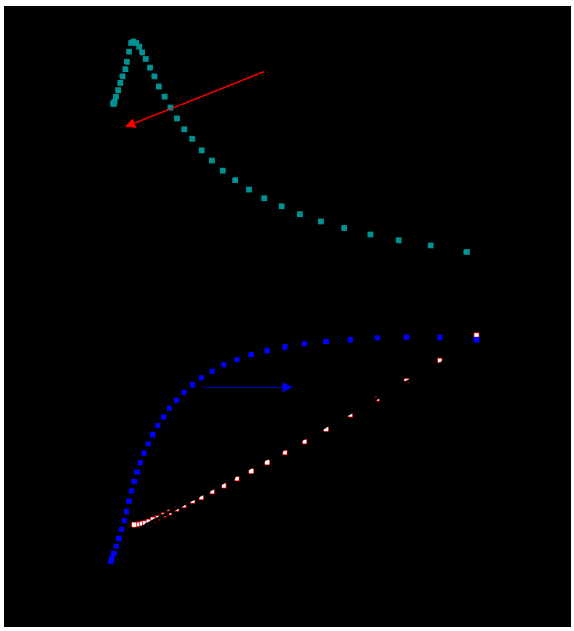

Figure 1. a) Magnetic susceptibility data of 15%Cu@ZIF-67. b) Plot of $\chi_P T$ vs. T (blue) and a Curie plot (red) for 15%Cu@ZIF-67. The least-squares fit(black) over the quasi-linear region of the Curie plot is superimposed on the red trace.

to previously reported post-synthetic metal substation methods.[28-30] This innovative approach allowed the incorporation of a relatively larger content of guest metals in a controlled manner before the dissolution of the parent materials. The concentration of each metal node in the mixed-metal ZIFs was confirmed by ICP-MS (Table S1). The XRD patterns and X-ray absorption spectra (XAS) at the Co K-edge of these mixed-metal ZIFs resemble that of the parent ZIFs (Figures S1-3), indicating that the incorporation of guest metals has a negligible effect on the crystal structure of the parent ZIFs. The coordination environment at the guest metal center was determined to be tetrahedral by XAS (Figures S4-5). The tetrahedral environment at Cu^{2+} centers in Cu@ZIF-67 was further supported by its reflective UV-Visible-NIR spectra (Figure S6), where two prominent absorption bands are observed at 400-580 nm and 600-1600 nm, corresponding to ligand-to-metal charge transfer and Cu d-d transitions in a tetrahedral ligand field, respectively.[31-34]

The ground state interaction among metal nodes in mixed-metal ZIFs was investigated by SQUID magnetometry. As shown in Figure 1a (representative data set for 15%Cu@ZIF-67) and Figure S7, the paramagnetic susceptibility data for ZIF-67 and all Cu@ZIF-67 samples all exhibit a transition to an antiferromagnetically ordered state at temperatures lower than ~21 K (T_N). Below T_N, thermal energy is insufficient to disrupt the long-range order that causes all neighboring spins to cancel each other,[35] which is antiferromagnetic behavior. Figure 1b shows the plot of $\chi_P T$ vs. T and a Curie plot for 15%Cu@ZIF-67. The observed curvature in the plot of $\chi_P T$ vs. T above T_N is characteristic of the $^4A_2$ state of tetrahedral Co^{2+}. The antiferromagnetism of the ZIF samples is quantified by the Weiss constants, Θ, (SI, Table S2), derived from the x-intercepts of the Curie plots. The Θ values range from −29 to −32 K regardless of the amount of Cu doping. Control experiments with Zn-doped ZIF-67 samples were also conducted (Figure S9). Comparing the data for ZIF-67, 15%Zn@ZIF-67, and 15%Cu@ZIF-67 shows antiferromagnetic ordering only in the 100%Co and 15%Cu samples (Figure S8). Inclusion of Zn^{2+} shuts down the magnetic exchange interactions responsible for the ordering behavior, while inclusion of Cu^{2+} enforces the magnetic ordering.

To examine the charge transport nature of ZIFs, we first investigated the effect of redox inert metals (Zn^{2+}) on ECS dynamics using OTA spectroscopy. Two ZIF model systems, 80%Zn@ZIF-67 and 50%Zn@ZIF-67, were studied. While these samples are isostructural with ZIF-67 parent framework, the UV-visible-NIR spectra show decreasing absorption of both Co d-d and LMCT transitions (Figure 2a) with increasing Zn^{2+} content due to the dilution of the Co^{2+} chromophores by the non-absorbing Zn^{2+} with a $3d^{10}$ electron configuration. This is also reflected in their OTA spectra following the excitation of the lower lying Co^{2+} d-d transition ($^4A_2(F)$-$^4T_1(F)$) at 1000 nm, where the intensity of OTA spectra decreases significantly with increasing content of Zn^{2+} (Figure 2b and S10). Nevertheless, the shape of the OTA spectra, featured by a ground state bleach (GSB) at 585 nm and positive absorption at both sides of the GSB, remains similar among the mixed-metal ZIFs. These spectral signatures are consistent with the derivative feature observed previously in ZIF-67[20] and can thus be assigned to the formation of a long-lived ECS state in Zn@ZIF-67. Despite the formation of the ECS state in Zn@ZIF-67, significant differences were observed when we compared their kinetic traces, where the recovery of the GSB became faster (inset of Figure 2c) while the formation of the ECS state is slower in the films with higher Zn^{2+} content (Figure 2c). Because of the closed-shell configuration of Zn^{2+}, it is unlikely that MMCT would occur from Co^{2+} to Zn^{2+}. Instead, these results can be well explained by a model proposed in the inset of Figure 2a: the presence of a statistical number of Zn^{2+} neighbors with closed-shell configuration partially blocks the inherent ECS pathway in ZIF-67 through Co-Co communication, resulting in slower formation of the ECS state. As a result, direct transition from $^4T_1$ to $^4A_2$ is facilitated, which leads to faster GSB recovery kinetics.

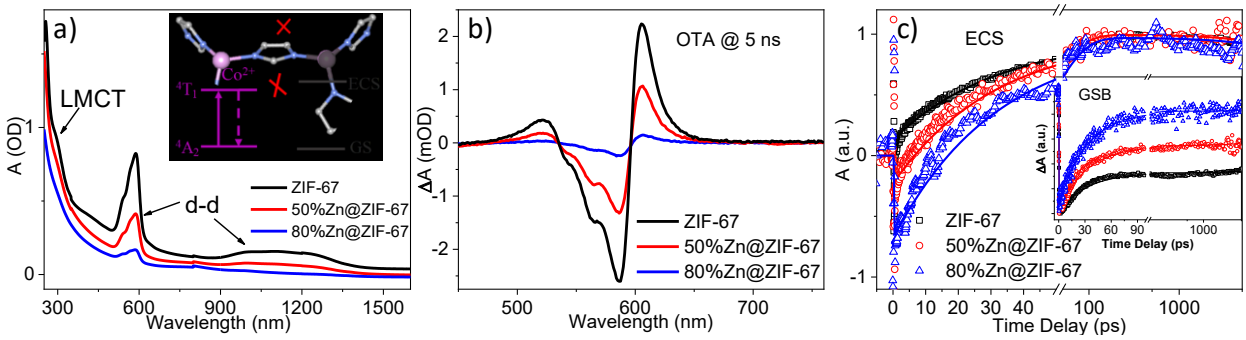

Figure 2. (a) UV-visible-NIR absorption spectra of Zn^{2+} incorporated ZIF-67 with different Zn percent (X%Zn@ZIF-67). The inset shows the proposed schematic model for prevented formation of the ECS in the X%Zn@ZIF-67 model system. b) The OTA spectra of X%Zn@ZIF-67 at 5 ns time delay following 1000 nm excitation. (c) The comparison of kinetics of ESC absorption at 610 nm and GSB recovery at 585nm (inset).

While the experiments with Zn@ZIF-67 model systems show that the presence of Zn^{2+} can partially block Co-Co communication (which suggests that metal-to-metal communication is likely responsible for the long-lived ECS state in ZIF-67), it is necessary to provide direct evidence to confirm this mechanism. To do so, we designed a second model system, where open-shell Cu^{2+} ions are used as guest metals to replace Co^{2+} centers in ZIF-67 (X%Cu@ZIF-67). The OTA spectra show that X%Cu@ZIF-67 samples with variable Cu content can also form a long-lived ECS state (Figure S11), where the lifetime for ECS formation (Figure 3a) and GSB recovery (Figure 3b) remains similar to that of the parent ZIF, suggesting that the presence of redox-active Cu^{2+} does not inhibit ECS state formation. To evaluate the interaction between Cu and Co in X%Cu@ZIF-67, we utilized X-ray transient absorption (XTA) spectroscopy, a powerful element-specific time-resolved technique, to directly probe the electron density changes at the Cu^{2+} centers following selective excitation of the Co^{2+} centers. XTA experiments at the Cu K-edge were performed using 590 nm excitation, where Co^{2+} d-d transitions are at a maximum absorbance and Cu^{2+} d-d transitions have negligible absorption (for tetrahedral ligand fields). Figure 3c shows the XANES spectrum of 15%Cu@ZIF-67 at the Cu K-edge, which features a strong white line absorption corresponding to the Cu 1s-4p transition. Also shown in Figure 3c is the difference spectra obtained after subtracting the ground state XANES spectrum from the spectrum collected at delay times at 120 ps and 500 ps following laser excitation, which demonstrates the transient signals of Cu due to excitation of Co. A clear positive feature was observed at ~ 8.99 keV, which overlaps with the 1s-4p transition edge, indicating that the edge energy of Cu shifts to lower energy. Because no transient signal (lower set in Figure 3c) was observed in the 17%Cu@ZIF-8 control sample (inert parent framework with Zn^{2+} node), we can rule out the possibility that the observed Cu edge shift in 15%Cu@ZIF-67 is due to direct excitation of Cu^{2+} centers. As a result, we can conclude that the reduction of Cu arises from the excitation of Co, unambiguously demonstrating a metal-to-metal charge transport mechanism through node-to-node communication in X%Cu@ZIF-67, although the degree of charge delocalization remains uncertain to us. It is also important to note that while the proposed model resembles an electron hopping mechanism, a band transport mechanism may contribute to charge migration in ZIFs.

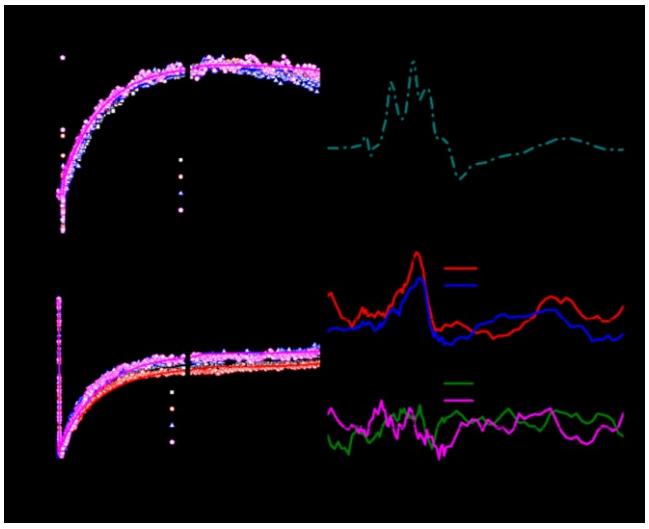

Figure 3. Kinetic traces of the ESC state at 610 nm (a) and the GSB at 585 nm (b) for ZIF-67 and Cu@ZIF-67 with variable % Cu. (c) Representative Cu K-edge XAS spectrum (black, XA) and first derivative spectrum, XTA difference spectra at the Cu K-edge for Cu@ZIF-67 (top set) and Cu@ZIF-8 (bottom set) after 590 nm excitation at 120 and 500 ps time delays.

In summary, we have reported for the first time the charge transport properties of ZIFs using a combination of multiple spectroscopic methods. We designed two mixed-metal ZIFs by incorporating a guest metal (Zn^{2+} or Cu^{2+}) to the ZIF-67 parent framework and directly probed the interaction between the guest metals and the metal centers in the parent framework. The paramagnetic susceptibility measurements on both ZIF-67 and Cu@ZIF-67 indicate the presence of intrinsic antiferromagnetic ordering of metal nodes, demonstrating ground-state quantum level communication between Co^{2+}/Co^{2+} and Co^{2+}/Cu^{2+} nodes. Using optical transient absorption spectroscopy, we found that replacing Co^{2+} with closed-shell Zn^{2+} retarded the formation of an ECS state after Co^{2+} d-d excitation, suggesting the presence of Co-Co communication in ZIF-67 and charge delocalization within the long-lived ECS state. In contrast, when a redox active metal, Cu^{2+}, is introduced into ZIF-67, we directly observed the migration of charge from photoexcited Co^{2+} to Cu^{2+} centers using X-ray transient absorption (XTA) spectroscopy, unambiguously confirming the charge transport pathway through node-to-node communication between different units of ZIFs. These findings not only advance the scientific understanding of the optical and electrical properties of ZIFs, paving the way for their novel application in photoenergy conversion, but also demonstrate an original approach to study porous ZIFs at the molecular level using spectroscopic techniques. Moving forward, computational studies

on the excited state electronic structures are necessary to gain further information on the charge transport mechanism in ZIFs.

ASSOCIATED CONTENT

Supporting Information

The Supporting Information is available free of charge on the ACS Publications website. Experimental details, structural and optical characterization data, and supplementary SQUID, XAS, and OTA figures.

AUTHOR INFORMATION

Corresponding Author

*Jier Huang (jier.huang@marquette.edu)
*John F. Berry (berry@chem.wisc.edu)

Notes

The authors declare no competing financial interests.

ACKNOWLEDGMENT

This work was supported by National Science Foundation (DMR-1654140) and ACS-PRF (57503-DNI6). Use of the Advanced Photon Source at Argonne National Laboratory was supported by the U. S. Department of Energy, Office of Science, Office of Basic Energy Sciences, under Award No. DE-AC02-06CH11357.

REFERENCES

(1) Scholes, G. D.; Fleming, G. R.; Olaya-Castro, A.; van Grondelle, R. *Nat. Chem.* **2011**, *3*, 763.
(2) Maza, W. A.; Padilla, R.; Morris, A. J. *J. Am. Chem. Soc.* **2015**, *137*, 8161.
(3) Furukawa, H.; Cordova, K. E.; O'Keeffe, M.; Yaghi, O. M. *Science* **2013**, *341*, 974.
(4) Zhang, T.; Lin, W. B. *Chem. Soc. Rev.* **2014**, *43*, 5982.
(5) Wang, J.-L.; Wang, C.; Lin, W. *ACS Catal.* **2012**, *2*, 2630.
(6) Zhou, H.-C.; Long, J. R.; Yaghi, O. M. *Chem. Rev.* **2012**, *112*, 673.
(7) Lu, W.; Wei, Z.; Gu, Z.-Y.; Liu, T.-F.; Park, J.; Park, J.; Tian, J.; Zhang, M.; Zhang, Q.; Gentle Iii, T.; Bosch, M.; Zhou, H.-C. *Chem. Soc. Rev.* **2014**, *43*, 5561.
(8) Cohen, S. M. *Chem. Rev.* **2012**, *112*, 970.
(9) Kent, C. A.; Liu, D.; Meyer, T. J.; Lin, W. *J. Am. Chem. Soc.* **2012**, *134*, 3991.
(10) Son, H. J.; Jin, S. Y.; Patwardhan, S.; Wezenberg, S. J.; Jeong, N. C.; So, M.; Wilmer, C. E.; Sarjeant, A. A.; Schatz, G. C.; Snurr, R. Q.; Farha, O. K.; Wiederrecht, G. P.; Hupp, J. T. *J. Am. Chem. Soc.* **2013**, *135*, 862.
(11) Kent, C. A.; Mehl, B. P.; Ma, L. Q.; Papanikolas, J. M.; Meyer, T. J.; Lin, W. B. *J. Am. Chem. Soc.* **2010**, *132*, 12767.
(12) Zhang, Z.-M.; Zhang, T.; Wang, C.; Lin, Z.; Long, L.-S.; Lin, W. *J. Am. Chem. Soc.* **2015**, *137*, 3197.
(13) Maza, W. A.; Morris, A. J. *J. Phys. Chem. C* **2014**, *118*, 8803.
(14) Yang, S.; Fan, D.; Hu, W.; Pattengale, B.; Liu, C.; Zhang, X.; Huang, J. *J. Phys. Chem. C* **2018**, *122*, 3305.
(15) Lee, C. Y.; Farha, O. K.; Hong, B. J.; Sarjeant, A. A.; Nguyen, S. T.; Hupp, J. T. *J. Am. Chem. Soc.* **2011**, *133*, 15858.
(16) Phan, A.; Doonan, C. J.; Uribe-Romo, F. J.; Knobler, C. B.; O'Keeffe, M.; Yaghi, O. M. *Acc. Chem. Res.* **2010**, *43*, 58.
(17) Chen, B. L.; Yang, Z. X.; Zhu, Y. Q.; Xia, Y. D. *J. Mater. Chem. A* **2014**, *2*, 16811.
(18) Park, K. S.; Ni, Z.; Côté, A. P.; Choi, J. Y.; Huang, R.; Uribe-Romo, F. J.; Chae, H. K.; O'Keeffe, M.; Yaghi, O. M. *Proc. Natl. Acad. Sci. U.S.A.* **2006**, *103*, 10186.
(19) Pattengale, B.; Yang, S. Z.; Lee, S.; Huang, J. *ACS Catal.* **2017**, *7*, 8446.
(20) Pattengale, B.; Yang, S.; Ludwig, J.; Huang, Z.; Zhang, X.; Huang, J. *J. Am. Chem. Soc.* **2016**, *138*, 8072.
(21) Yang, S. Z.; Pattengale, B.; Kovrigin, E. L.; Huang, J. *ACS Energy Lett.* **2017**, *2*, 75.
(22) Pattengale, B.; Huang, J. *Phys. Chem. Chem. Phys.* **2018**, *20*, 14844.
(23) Butler, K. T.; Hendon, C. H.; Walsh, A. *ACS Appl. Mater. Interfaces* **2014**, *6*, 22044.
(24) Grau - Crespo, R.; Aziz, A.; Collins, A. W.; Crespo - Otero, R.; Hernández, N. C.; Rodriguez - Albelo, L. M.; Ruiz - Salvador, A. R.; Calero, S.; Hamad, S. *Angew. Chem. Int. Ed.* **2016**, *55*, 16012.
(25) Butler, K. T.; Hendon, C. H.; Walsh, A. *J. Am. Chem. Soc.* **2014**, *136*, 2703.
(26) Sun, L.; Campbell, M. G.; Dincă, M. *Angew. Chem. Int. Ed.* **2016**, *55*, 3566.
(27) Butler, K. T.; Worrall, S. D.; Molloy, C. D.; Hendon, C. H.; Attfield, M. P.; Dryfe, R. A. W.; Walsh, A. *J. Mater. Chem. C* **2017**, *5*, 7726.
(28) Fei, H. H.; Cahill, J. F.; Prather, K. A.; Cohen, S. M. *Inorg. Chem.* **2013**, *52*, 4011.
(29) Ban, Y. J.; Li, Y. S.; Peng, Y.; Jin, H.; Jiao, W. M.; Liu, X. L.; Yang, W. S. *Chem. Eur. J.* **2014**, *20*, 11402.
(30) Schejn, A.; Aboulaich, A.; Balan, L.; Falk, V.; Lalevee, J.; Medjahdi, G.; Aranda, L.; Mozet, K.; Schneider, R. *Catal. Sci. Technol.* **2015**, *5*, 1829.
(31) Shimizu, I.; Morimoto, Y.; Faltermeier, D.; Kerscher, M.; Paria, S.; Abe, T.; Sugimoto, H.; Fujieda, N.; Asano, K.; Suzuki, T.; Comba, P.; Itoh, S. *Inorg. Chem.* **2017**, *56*, 9634.
(32) Casella, L.; Carugo, O.; Gullotti, M.; Doldi, S.; Frassoni, M. *Inorg. Chem.* **1996**, *35*, 1101.
(33) Solomon, E. I. *Inorg. Chem.* **2006**, *45*, 8012.
(34) Hoffmann, S. K.; Goslar, J.; Lijewski, S.; Zalewska, A. *J. Magn. Resn.* **2013**, *236*, 7.
(35) Carlin, R. L. *Magnetochemistry*; Springer-Verlag: Berlin New York, 1986.